

Overcoming temperature limits in the optical cooling of solids using light-dressed states

Conor N. Murphy, Luísa Toledo Tude and Paul R. Eastham
School of Physics, Trinity College Dublin, Dublin 2, Ireland
(Dated: September 30, 2022)

Laser cooling of solids currently has a temperature floor of 50–100 K. We propose a method that could overcome this using defects, such as diamond color centers, with narrow electronic manifolds and bright optical transitions. It exploits the dressed states formed in strong fields which extend the set of phonon transitions and have tunable energies. This allows an enhancement of the cooling power and diminishes the effect of inhomogeneous broadening. We demonstrate these effects theoretically for the silicon vacancy and discuss the role of background absorption and non-radiative decay.

The optical cooling of solids to low temperatures is an important open challenge. The current method [1–3] is anti-Stokes fluorescence in rare-earth doped glasses [4]. In this process a rare-earth ion absorbs light, creating an excited electronic state which then absorbs phonons before re-emitting the light at a higher frequency. Despite the competing heating by non-radiative decay and background absorption, temperatures as low as 91K have been reached [3]. This is, however, reaching the fundamental limit of 50-100K [4] set by the phonon energy that can be effectively absorbed. The same issue of a characteristic phonon energy also limits the possible cooling by absorption of optical phonons reported in room-temperature semiconductors [5, 6] (see also Ref. [7]), and while various techniques have been considered to improve performance along with different cooling schemes [2, 3, 6, 8–10], they do not address this problem. One route to reaching lower temperatures exploits the continuous electronic dispersion in semiconductors [11–15], but has yet to be achieved [7].

In this Letter, we propose a mechanism by which the temperature floor of solid-state laser cooling could be overcome, using quasi-resonant excitation of a suitable defect state. We focus on the group IV color centers in diamond and in particular the negatively charged Silicon-Vacancy defect (SiV). The states of this defect comprise a ground-state and an excited-state manifold with dipole-active optical transitions between the two [16–19]. At sufficiently low temperatures the optical spectrum shows four lines, two of which could be resonantly driven to produce a form of anti-Stokes cooling. For weak driving this process is very sensitive to detuning. However, for stronger driving the dynamics becomes controlled by laser-dressed states rather than the original electronic eigenstates. The formation of these states, via the Autler-Townes/a.c. Stark effect [20], leads to a more complex cooling process with many phonon transitions occurring within the dressed-state spectrum. This process, which we dub Dressed state Anti-Stokes Cooling (DASC), corresponds to the inelastic scattering of the driving laser in the strong-driving regime. Importantly, it can be tuned to optimise the phonon absorption rates:

by controlling the field intensity and detuning, the energy gaps and phonon matrix elements are modified in such a way that the coupling to the phonons is larger for the most occupied states at a given temperature. For the SiV we predict high gross cooling powers, of 1-100 fW per defect, down to temperatures of a few Kelvin. This is many orders-of-magnitude greater than could be achieved using rare-earth ions, even at the higher temperatures where they can operate. Furthermore, the cooling effect occurs over a broad range of detunings (see Fig. 1), and so survives in the presence of inhomogeneous broadening. While it will compete with heating due to non-radiative decay and background absorption, our results suggest that DASC could enable the optical cooling of solids to temperatures unachievable with existing methods.

The SiV in diamond [18] is one of a family of group IV color centres [19] that are candidates for DASC. They are of interest for quantum nanophotonics, acting as both optically addressable spin qubits and effective single-photon emitters [21]. The electronic and spin states have long coherence times in the low temperature regime we consider, producing lifetime-limited spectra without spectral diffusion [18]. The spin coherence time for the SiV is sub-microsecond due to phonon scattering within the ground-state manifold [18]. While this is disadvantageous for use as a spin qubit, it is beneficial for cooling because it allows rapid phonon absorption. While some group IV defects, in particular the Germanium vacancy, have high quantum efficiencies [22], the SiV has a relatively low quantum efficiency measured in photoluminescence [17]. Although this could be problematical for cooling in general, it would not affect DASC if, as suggested by the electronic structure [23, 24], it is due to higher energy states. Conventional anti-Stokes cooling using the SiV and related Nitrogen Vacancy (NV) was considered in recent works [25, 26], based on the broad absorption lines observed at room temperature. Here we consider, instead, high quality materials at low temperatures, where individual spectral lines are resolved. This opens up the possibility of precision cooling approaches with tailored excitation of well-characterized transitions. Methods for

cooling micromechanical resonators using the NV and SiV have been proposed [27, 28], however, the goal in that case is to cool a single resonator mode, whereas we consider cooling of the bulk material.

To study optical cooling using a SiV we use an open-quantum systems description based on the Born-Markov approximation. As usual, we divide the problem into a system and baths, with the system Hamiltonian describing the SiV driven by a laser. It is a one-hole system with eight levels, four associated with spin-up and four with spin-down. The levels in each spin sector form an excited (u) and ground (g) state manifold, each containing two levels. The states in each manifold, $|u_{\pm}\rangle$ and $|g_{\pm}\rangle$, are split by the spin-orbit coupling constants $\lambda^u = 1.11$ meV and $\lambda^g = 0.19$ meV [16]. We ignore the small contribution of the linear vibronic Jahn-Teller interaction, which is around 5% of the spin-orbit coupling and so would not qualitatively affect our results. The manifolds are separated by the zero phonon line energy $E_{ZPL} = 1.68$ eV, and coupled by electric-dipole optical transitions of various polarizations. We suppose that these transitions are driven by lasers of a single frequency ω_l , and use the Floquet basis obtained after a unitary transformation $U = e^{i\omega_l t(|u_+\rangle + |u_-\rangle)}$. The Hamiltonian for the spin-down sector is, with $\hbar = 1$,

$$H_S = \frac{1}{2} \begin{pmatrix} -\Delta + \lambda^u & 0 & \Omega_z & \Omega_+ \\ 0 & -\Delta - \lambda^u & \Omega_- & \Omega_z \\ \Omega_z & \Omega_- & \Delta + \lambda^g & 0 \\ \Omega_+ & \Omega_z & 0 & \Delta - \lambda^g \end{pmatrix}. \quad (1)$$

The basis here is in the order of decreasing energy in the original frame. In the Floquet basis the energies are shifted by the laser frequency, and given in terms of the detuning from the zero-phonon line $\Delta = \omega_l - \omega_{ZPL}$. Ω_z is the Rabi frequency quantifying the strength of the driving with polarization along the z-axis, which is the [111] crystal axis, and Ω_{\pm} are the Rabi frequencies for the two circular polarizations in the xy plane. The Hamiltonian for the spin-up sector is identical, except that the two circular polarizations are swapped. Most of our results refer to situations where $\Omega_+ = \Omega_-$, so that H_S describes both spin sectors.

Acoustic phonons cause transitions between states in each manifold due to the intramanifold coupling [28]

$$H_{I1} = \sum_k (f_k^u |u_+\rangle \langle u_-| + f_k^g |g_+\rangle \langle g_-|) \otimes a_k + \text{H.c.} \quad (2)$$

They also affect the energy separation of the manifolds due to the intermanifold deformation-potential coupling [29, 30]

$$H_{I2} = \sum_k g_k (|u_+\rangle \langle u_+| + |u_-\rangle \langle u_-| - |g_+\rangle \langle g_+| - |g_-\rangle \langle g_-|) \otimes (a_k + a_k^\dagger). \quad (3)$$

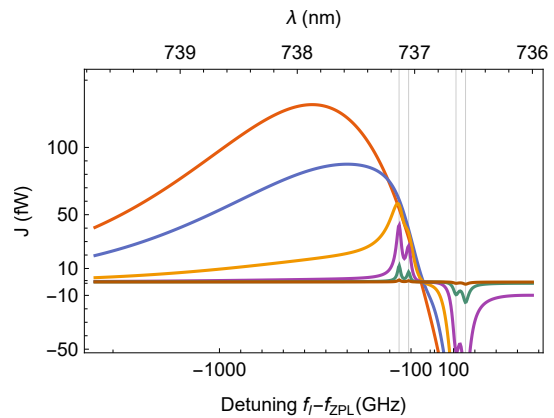


FIG. 1. Calculated cooling power of a single laser-driven SiV at $T = 20$ K, as a function of laser detuning. Different curves correspond to the different Rabi frequencies, i.e., driving strengths, $\Omega = 2 \times 10^{-0.5}, 2 \times 10^{-1}, \dots, 2 \times 10^{-3}$ rad ps $^{-1}$. Rabi frequency decreases from the top to the bottom curves on the left of the plot. All polarizations are driven equally, $\Omega_z = \Omega_+ = \Omega_- = \Omega$. The vertical lines mark the four transitions between the ground-state and excited-state manifolds.

The phonons have a super-Ohmic spectral density; we take the form [29, 30] $J(\omega) = 2A\omega_c^{-2}\omega^3 e^{-\omega/\omega_c}$ with $A = 0.0275$ and $\omega_c = 2\pi$ rad ps $^{-1}$. We include only the bulk phonon contribution relevant to our results, neglecting the local phonons which have much higher energies. The intermanifold coupling has been modelled [28] using the same form of $J(\omega)$ but with $A = 0.073$, reflecting the difference in matrix elements. We include this difference in the ratio f_k^u/g_k and for simplicity take $f_k^u = f_k^g$.

An equation-of-motion for the reduced density matrix of the SiV can be obtained using the Born-Markov approximation [31], which is well justified in the parameter regimes we consider. The general form we use here is given in [32], where we also present the general form for the mean heat current obtained using the method of full counting statistics [33]. In our case this heat current J is that from the phonons to the SiV. We include the radiative decays using standard Lindblad dissipators [31], one for each transition from one of the u states to one of the g states. We neglect differences in the rates of the different decays, which are factors of order one, and take them all to have rate $\gamma_0 = 1$ ns $^{-1}$ [34, 35]. We drop the Lamb shift terms, which are negligible, but do not make the secular approximation. Although it would be valid for strong driving, it fails for weak resonant driving, and we wish to treat both regimes. We note that although it has been argued to be necessary [36, 37], calculations without it nonetheless give accurate results [32, 38–40].

Fig. 1 shows the calculated cooling power as a function of driving frequency, for a single SiV at a temperature of 20K, driven with $\Omega_z = \Omega_+ = \Omega_-$. Different curves correspond to different driving strengths. At weak driving, we see two characteristic peaks on each side of zero de-

tuning, with those on the red (blue) side corresponding to net cooling (heating) of the phonons. The cooling (heating) effect corresponds to weak resonant driving of the two lowest (highest) of the four lines in the optical spectrum. As the driving is increased the red-detuned features first evolve into a broad spectral region where there is a very high cooling power. Further increases, beyond the driving strengths shown, then lead to a reduction in the maximum power.

To explain these phenomena we show in Fig. 2 the energy levels for H_S and the breakdown of the heat current into contributions from each pair of levels, for two different driving strengths and detunings. Here we have taken only Ω_- to be non-zero. Panels (a) and (c) illustrate the behavior for weak driving resonant with the lowest-energy optical transition, from $|g_+\rangle$ to $|u_-\rangle$. In the Floquet basis these levels are degenerate, and weakly coupled by the driving laser. This does not produce a noticeable energy splitting, and its effect is merely to transfer population between the states. This leads to an anti-Stokes-type cooling cycle operating with the unperturbed states: phonons are absorbed in transitions within each manifold, and the cycle is closed by absorption of laser photons and radiative decay. The dominant contribution to the cooling power at this temperature comes from phonon absorption in the upper manifold, because the rate is proportional to the product of the spectral density and phonon occupation, $J(\omega)n(\omega)$, which is larger at the transition energy λ^u than at λ^g . In this weak driving regime the energy shifts and line broadenings are small, and cooling only occurs close to resonance.

The behaviour for stronger driving, below the lowest-energy transition, is exemplified in Fig. 2b. This diagram shows the original energy levels in the Floquet basis, as well as the energy levels of H_S . The states $|u_-\rangle$ and $|g_+\rangle$ are strongly mixed by the driving field, to form dressed-states $|D_\pm\rangle = \beta|u_-\rangle \pm \alpha|g_+\rangle$, with energies shifted as in the Autler-Townes effect. This mixing allows direct single-phonon processes which do not occur otherwise, for example, from the state nearest in energy to $|g_+\rangle$, $|D_-\rangle$, to the state $|u_+\rangle$, which can occur via H_{I1} given the admixture of $|u_-\rangle$ in $|D_-\rangle$. This mixing also leads to effects due to the deformation-potential interaction H_{I2} , which causes phonon transitions between the dressed states $|D_\pm\rangle$. This type of process has previously been predicted to allow cooling with quantum-dot excitons [41, 42], though in our case it provides only a small fraction of the heat current. As can be seen in Fig. 2d, the larger heat current compared with the weak driving case is mostly due to the increase in number and power of the transitions involving H_{I1} . This reflects the better match between the splittings in the strong-driving spectrum and the product $J(\omega)n(\omega)$. Furthermore, since significant mixing occurs for driving within a detuning $\sim \Omega$ of a resonance, the cooling effect does not require exact resonance and will survive some inhomogeneous broad-

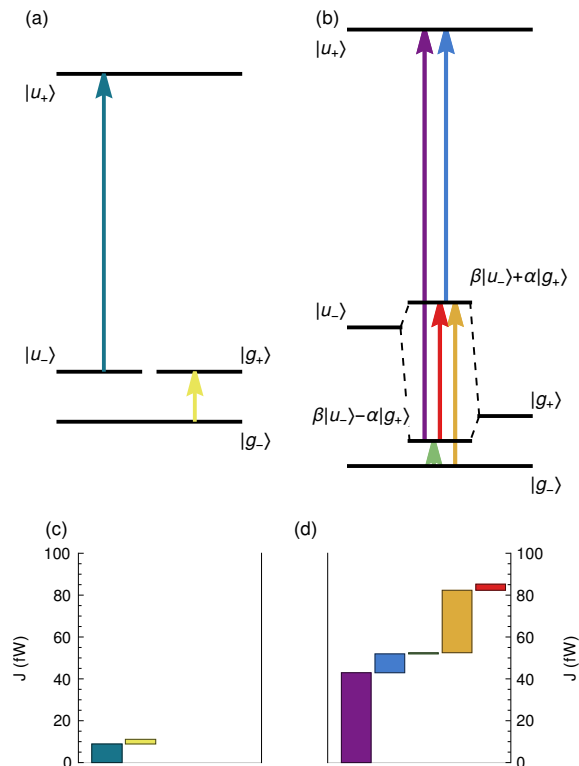


FIG. 2. Energy levels of the Floquet states (top row), and associated heat currents for each pair of levels (bottom row) for weak resonant driving (left column), and strong driving (right column). For weak driving the energy levels are unaffected, and phonon cooling occurs via transitions between the unperturbed states. Strong driving gives the energies shown in the central part of panel (b), which are shifted relative to the undriven case (outer parts). Phonon cooling occurs via transitions between laser-dressed states formed from admixtures of the original levels. $\Omega_+ = \Omega_z = 0$. Left column: $\Omega_- = 2 \times 10^{-2}$ rad ps $^{-1}$, with driving on the $|g_+\rangle \rightarrow |u_-\rangle$ transition. Right column: $\Omega_- = 3 \times 10^{-1}$ rad ps $^{-1}$, with driving 80 GHz below the transition.

ening.

Figure 3 shows the calculated maximum cooling power, obtained by maximizing over the detuning, as a function of temperature. We also show the corresponding values of the detuning. For weak driving, the optimal detuning is indistinguishable from that of the $|g_+\rangle \rightarrow |u_-\rangle$ transition, $-(\lambda^u + \lambda^g)/2$. The cooling power starts at zero and initially increases, before remaining constant for $T \gtrsim 10K \approx \lambda^u/k$. This saturation reflects the existence of a characteristic energy λ^u that can be absorbed per cycle at weak driving. In contrast, for strong driving the dressed-state spectrum contains transitions at the typical phonon energy $\sim kT$, allowing a high cooling rate and a linear temperature dependence at the higher temperatures shown. As this indicates, the benefit of strong driving is not in enhancing the cooling below the temper-

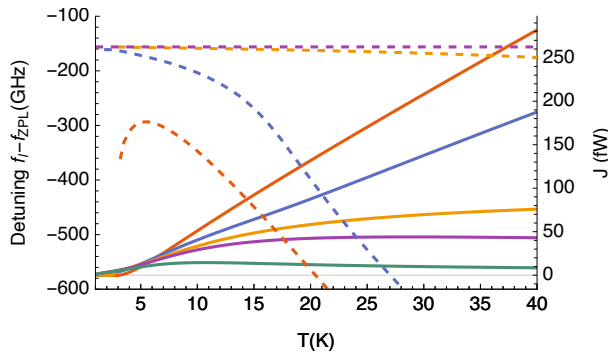


FIG. 3. Maximum cooling power (solid curves, right axis) and corresponding detuning (dashed curves, left axis) as a function of temperature for several different driving strengths. Results are shown for $\Omega_z = \Omega_+ = \Omega_- = 2 \times 10^{-0.5}, 2 \times 10^{-1}, \dots, 2 \times 10^{-2.5}$ rad ps $^{-1}$. The smallest Rabi frequency corresponds to the smallest power on the right of the plot, and the largest (least negative) detuning. The detuning curves for the two smallest Rabi frequencies coincide.

ature scale set by the undressed gap. Rather, it would be in allowing systems with smaller gaps, such as the SiV, to be used effectively above that temperature.

The cooling will compete with heating due to background absorption in the host material. The Rabi frequency $\hbar\Omega = dE_0$, where d is the transition dipole moment and E_0 the electric field amplitude, and the intensity is $I = c\epsilon_0 n E_0^2 / 2$. The heating rate per vacancy is then $c\epsilon_0 n \hbar^2 \Omega^2 \alpha / (2d^2 \rho)$, where α is the absorption coefficient and ρ the vacancy density. Considering the strongest field used in Fig. 1, we have a heating power $\sim 10^{25}(\alpha/\rho)$ fW m $^{-2}$, against a cooling power of ~ 100 fW. Taking a conservative absorption coefficient $\alpha = 0.1$ cm $^{-1}$ [43], and $d = 14.3$ Debye [18] we then predict net cooling for $\rho \gtrsim 10^{24}$ m $^{-3}$, or about one SiV per 10^5 carbon atoms. Thus background heating is unlikely to be a limitation.

Another competing heating effect will arise from any non-radiative decay from the u to the g manifold. The impact of this will be similar to that in conventional laser cooling [4]. The cooling power is limited by the radiative decay rate, and hence is on the order of $kT\gamma_0 p_u$, where p_u is the probability of occupying the upper manifold. A non-radiative decay to the g manifold with rate γ_{NR} will produce heating of $E_{ZPL}\gamma_{NR}p_u$, so that cooling dominates at 10 K if $\gamma_0/\gamma_{NR} > E_{ZPL}/kT \gtrsim 1000$. The implied quantum efficiency (QE) of 99.9% is far in excess of the values typically reported for SiVs [17]. However, these values refer to photoluminescence, and hence include non-radiative losses associated with states at higher energies than those relevant here. When driving below

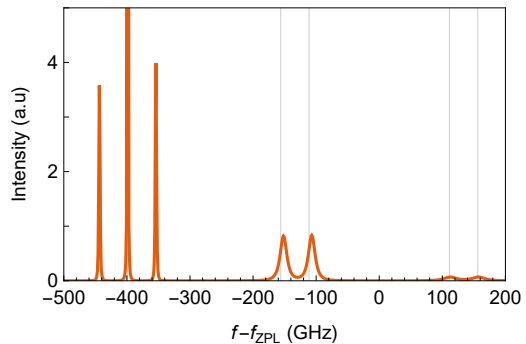


FIG. 4. Computed spectrum of the light from an SiV at 20K driven with $\Omega_+ = \Omega_- = \Omega_z = 2 \times 10^{-1}$ rad ps $^{-1}$. This corresponds to the second highest driving shown in Fig. 1. The laser is detuned to the maximum in the cooling power at $f_l - f_{ZPL} = -400$ GHz. All polarization components have been combined to show the total power.

resonance only direct non-radiative decay or decay via lower-energy states contributes to γ_{NR} , and the relevant QE could be much higher. We note also promising recent results suggesting very high QEs for the Germanium vacancy [22].

Finally, we point out that the cooling process could be observed directly via the scattering of the driving laser. Fig. 4 shows the spectrum of the light from an SiV driven in the cooling regime. It contains two sidebands around the laser frequency, forming a Mollow triplet [44], and four broader peaks near the original emission lines. Consistent with the phonon heat currents in Fig. 4, the total intensity on the blue side of the laser exceeds that on the red side as heat is transferred from the phonons to the field.

In conclusion, we have proposed and analyzed an approach to the optical cooling of solids using quasi-resonant excitation of optically-active defect states. Our approach applies at temperatures where the defect states have narrow, well-resolved emission lines, and evolve coherently under laser driving. It could overcome the temperature limitations inherent in optical cooling using rare-earths, set by the width of the electronic manifolds E_{man} , by using laser dressing to enhance the cooling powers at temperatures $kT \gtrsim E_{\text{man}}$. This could allow systems with small E_{man} , such as the group-IV color centers in diamond, to nonetheless cool effectively. The dressed-state enhancement, along with the fast radiative rates, leads to predicted cooling powers many orders of magnitude greater than could be obtained using rare-earths, down to temperatures of a few Kelvin. An interesting question is the maximum temperature at which these processes could be effective. While the Born-Markov the-

ory will eventually break down, it is likely that the upper limit in practice will be set by the breakdown of the four-level model and the absorption and decay arising from other states.

We acknowledge funding from the Irish Research Council under award GOIPG/2017/1091.

-
- [1] R. I. Epstein, M. I. Buchwald, B. C. Edwards, T. R. Gosnell, and C. E. Mungan, Observation of laser-induced fluorescent cooling of a solid, *Nature* **377**, 500 (1995).
- [2] D. V. Seletskiy, S. D. Melgaard, S. Bigotta, A. Di Lieto, M. Tonelli, and M. Sheik-Bahae, Laser cooling of solids to cryogenic temperatures, *Nat. Photonics* **4**, 161 (2010).
- [3] S. D. Melgaard, A. R. Albrecht, M. P. Hehlen, and M. Sheik-Bahae, Solid-state optical refrigeration to sub-100 Kelvin regime, *Sci. Rep.* **6**, 20380 (2016).
- [4] D. V. Seletskiy, R. Epstein, and M. Sheik-Bahae, Laser cooling in solids: Advances and prospects, *Rep. Prog. Phys.* **79**, 096401 (2016).
- [5] J. Zhang, D. Li, R. Chen, and Q. Xiong, Laser cooling of a semiconductor by 40 Kelvin, *Nature* **493**, 504 (2013).
- [6] J. Zhang, Q. Zhang, X. Wang, L. C. Kwek, and Q. Xiong, Resolved-sideband Raman cooling of an optical phonon in semiconductor materials, *Nat. Photonics* **10**, 600 (2016).
- [7] Y. V. Morozov, S. Zhang, A. Pant, B. Jankó, S. D. Melgaard, D. A. Bender, P. J. Pauzauskie, and M. Kuno, Can lasers really refrigerate CdS nanobelts?, *Nature* **570**, E60 (2019).
- [8] N. Vermeulen, C. Debaes, P. Muys, and H. Thienpont, Mitigating heat dissipation in Raman lasers using coherent anti-Stokes Raman scattering, *Phys. Rev. Lett.* **99**, 093903 (2007).
- [9] S. C. Rand, Raman laser cooling of solids, *J. Lumin.* **133**, 10 (2013).
- [10] L. B. Andre, L. Cheng, and S. C. Rand, Saturation, allowed transitions and quantum interference in laser cooling of solids, *Appl. Sci.* **12**, 953 (2022).
- [11] M. Sheik-Bahae and R. I. Epstein, Can laser light cool semiconductors?, *Phys. Rev. Lett.* **92**, 247403 (2004).
- [12] L. A. Rivlin and A. A. Zadernovsky, Laser cooling of semiconductors, *Opt. Commun.* **139**, 219 (1997).
- [13] E. Finkeifen, M. Potemski, P. Wyder, L. Viña, and G. Weimann, Cooling of a semiconductor by luminescence up-conversion, *Appl. Phys. Lett.* **75**, 1258 (1999).
- [14] G. Rupper, N. H. Kwong, and R. Binder, Theory of semiconductor laser cooling at low temperatures, *Phys. Status Solidi C* **3**, 2489 (2006).
- [15] G. Rupper, N. H. Kwong, and R. Binder, Large excitonic enhancement of optical refrigeration in semiconductors, *Phys. Rev. Lett.* **97**, 117401 (2006).
- [16] C. Hepp, T. Müller, V. Waselowski, J. N. Becker, B. Pingault, H. Sternschulte, D. Steinmüller-Nethl, A. Gali, J. R. Maze, M. Atatüre, and C. Becher, Electronic structure of the silicon vacancy color center in diamond, *Phys. Rev. Lett.* **112**, 036405 (2014).
- [17] E. Neu, C. Hepp, M. Hauschild, S. Gsell, M. Fischer, H. Sternschulte, D. Steinmüller-Nethl, M. Schreck, and C. Becher, Low-temperature investigations of single silicon vacancy colour centres in diamond, *New J. Phys.* **15**, 043005 (2013).
- [18] J. N. Becker and C. Becher, Coherence properties and quantum control of silicon vacancy color centers in diamond, *Phys. Status Solidi A* **214**, 1700586 (2017).
- [19] C. Bradac, W. Gao, J. Forneris, M. E. Trusheim, and I. Aharonovich, Quantum nanophotonics with group IV defects in diamond, *Nat. Commun.* **10**, 5625 (2019).
- [20] S. H. Autler and C. H. Townes, Stark effect in rapidly varying fields, *Phys. Rev.* **100**, 703 (1955).
- [21] E. Neu, D. Steinmetz, J. Riedrich-Möller, S. Gsell, M. Fischer, M. Schreck, and C. Becher, Single photon emission from silicon-vacancy colour centres in chemical vapour deposition nano-diamonds on iridium, *New J. Phys.* **13**, 025012 (2011).
- [22] M. K. Bhaskar, D. D. Sukachev, A. Sipahigil, R. E. Evans, M. J. Burek, C. T. Nguyen, L. J. Rogers, P. Siyushev, M. H. Metsch, H. Park, F. Jelezko, M. Lončar, and M. D. Lukin, Quantum nonlinear optics with a germanium-vacancy color center in a nanoscale diamond waveguide, *Phys. Rev. Lett.* **118**, 223603 (2017).
- [23] S. Häußler, G. Thiering, A. Dietrich, N. Waasem, T. Teraji, J. Isoya, T. Iwasaki, M. Hatano, F. Jelezko, A. Gali, and A. Kubanek, Photoluminescence excitation spectroscopy of SiV⁻ and GeV⁻ color center in diamond, *New J. Phys.* **19**, 063036 (2017).
- [24] G. Thiering and A. Gali, Ab initio magneto-optical spectrum of group-IV vacancy color centers in diamond, *Phys. Rev. X* **8**, 021063 (2018).
- [25] M. Kern, J. Jeske, D. W. M. Lau, A. D. Greentree, F. Jelezko, and J. Twamley, Optical cryocooling of diamond, *Phys. Rev. B* **95**, 235306 (2017).
- [26] Y.-F. Gao, Q.-H. Tan, X.-L. Liu, S.-L. Ren, Y.-J. Sun, D. Meng, Y.-J. Lu, P.-H. Tan, C.-X. Shan, and J. Zhang, Phonon-assisted photoluminescence up-conversion of silicon-vacancy centers in diamond, *J. Phys. Chem. Lett.* **9**, 6656 (2018).
- [27] K. V. Kepesidis, S. D. Bennett, S. Portolan, M. D. Lukin, and P. Rabl, Phonon cooling and lasing with nitrogen-vacancy centers in diamond, *Phys. Rev. B* **88**, 064105 (2013).
- [28] K. V. Kepesidis, M.-A. Lemonde, A. Norambuena, J. R. Maze, and P. Rabl, Cooling phonons with phonons: Acoustic reservoir engineering with silicon-vacancy centers in diamond, *Phys. Rev. B* **94**, 214115 (2016).
- [29] A. Norambuena, J. R. Maze, P. Rabl, and R. Coto, Quantifying phonon-induced non-Markovianity in color centers in diamond, *Phys. Rev. A* **101**, 022110 (2020).
- [30] A. Norambuena, S. A. Reyes, J. Mejía-López, A. Gali, and J. R. Maze, Microscopic modeling of the effect of phonons on the optical properties of solid-state emitters, *Phys. Rev. B* **94**, 134305 (2016).
- [31] H.-P. Breuer and F. Petruccione, *The Theory of Open Quantum Systems* (Oxford University Press, 2007).
- [32] C. N. Murphy, L. Toledo Tude, and P. R. Eastham, Laser cooling beyond rate equations: Approaches from quantum thermodynamics, *Appl. Sci.* **12**, 1620 (2022).
- [33] M. Esposito, U. Harbola, and S. Mukamel, Nonequilibrium fluctuations, fluctuation theorems, and counting statistics in quantum systems, *Rev. Mod. Phys.* **81**, 1665 (2009).
- [34] H. Sternschulte, K. Thonke, R. Sauer, P. C. Münzinger, and P. Michler, 1.681-eV luminescence center in chemical-vapor-deposited homoepitaxial diamond films, *Phys. Rev. B* **50**, 14554 (1994).

- [35] C. Wang, C. Kurtsiefer, H. Weinfurter, and B. Burchard, Single photon emission from SiV centres in diamond produced by ion implantation, *J. Phys. B: At. Mol. Opt. Phys.* **39**, 37 (2005).
- [36] R. Dümcke and H. Spohn, The proper form of the generator in the weak coupling limit, *Z. Phys. B* **34**, 419 (1979).
- [37] J. O. González, L. A. Correa, G. Nocerino, J. P. Palao, D. Alonso, and G. Adesso, Testing the Validity of the ‘Local’ and ‘Global’ GKLS Master Equations on an Exactly Solvable Model, *Open Syst. Inf. Dyn.* **24**, 1740010 (2017).
- [38] J. Liu and D. Segal, Coherences and the thermodynamic uncertainty relation: Insights from quantum absorption refrigerators, *Phys. Rev. E* **103**, 032138 (2021).
- [39] P. R. Eastham, P. Kirton, H. M. Cammack, B. W. Lovett, and J. Keeling, Bath-induced coherence and the secular approximation, *Phys. Rev. A* **94**, 012110 (2016).
- [40] R. Hartmann and W. T. Strunz, Accuracy assessment of perturbative master equations: Embracing nonpositivity, *Phys. Rev. A* **101**, 012103 (2020).
- [41] E. M. Gauger and J. Wabnig, Heat pumping with optically driven excitons, *Phys. Rev. B* **82**, 073301 (2010).
- [42] C. N. Murphy and P. R. Eastham, Quantum control of excitons for reversible heat transfer, *Commun. Phys.* **2**, 120 (2019).
- [43] M. E. Thomas, Multiphonon model for absorption in diamond, in *SPIE’s 1994 International Symposium on Optics, Imaging, and Instrumentation*, edited by P. Klocek (San Diego, CA, 1994) pp. 152–159.
- [44] B. R. Mollow, Power spectrum of light scattered by two-level systems, *Phys. Rev.* **188**, 1969 (1969).